

Accepted Article

Title: Zinc Containing Small-Pore Zeolites for Capture of Low Concentration Carbon Dioxide

Authors: Donglong Fu, Youngkyu Park, and Mark Edward Davis

This manuscript has been accepted after peer review and appears as an Accepted Article online prior to editing, proofing, and formal publication of the final Version of Record (VoR). This work is currently citable by using the Digital Object Identifier (DOI) given below. The VoR will be published online in Early View as soon as possible and may be different to this Accepted Article as a result of editing. Readers should obtain the VoR from the journal website shown below when it is published to ensure accuracy of information. The authors are responsible for the content of this Accepted Article.

To be cited as: *Angew. Chem. Int. Ed.* 10.1002/anie.202112916

Link to VoR: <https://doi.org/10.1002/anie.202112916>

RESEARCH ARTICLE

Zinc Containing Small-Pore Zeolites for Capture of Low Concentration Carbon Dioxide

Donglong Fu, Youngkyu Park, and Mark E. Davis*

[*] Dr. D. Fu, Y. Park, Prof. Dr. M. E. Davis
 Chemical Engineering
 California Institute of Technology
 1200 E. California Blvd., Pasadena, CA 91125 (USA)
 E-mail: mdavis@cheme.caltech.edu

Supporting Information for this article is given via a link at the end of the document.

Abstract: The capture of low concentration CO₂ presents numerous challenges. Here, we report that zinc containing chabazite (CHA) zeolites can realize high capacity, fast adsorption kinetics, and low desorption energy when capturing ca. 400 ppm CO₂. Control of the state and location of the zinc ions in the CHA cage is critical to the performance. Zn²⁺ loaded onto paired anionic sites in the six-membered rings (6MRs) in the CHA cage are the primary sites to adsorb ca. 0.51 mmol CO₂/g-zeolite with Si/Al= ca. 7, a 17-fold increase compared to the parent H-form. The capacity is increased further to ca. 0.67 mmol CO₂/g-zeolite with Si/Al= ca. 2 due to more paired sites for zinc exchange. Zeolites with double six-membered rings (D6MRs) that orient 6MRs into the cages give enhanced uptakes for CO₂ adsorption with zinc exchange. The results reveal that zinc exchanged CHA and several other small pore, cage containing zeolites are worthy of further investigation for the capture of low concentration CO₂.

Introduction

Carbon dioxide (CO₂) capture is being investigated as an important approach to limit further increases in CO₂ concentration in the atmosphere.^[1] The conventional approaches for capturing high concentration (>10%) CO₂ are being developed for addressing emissions from point sources, such as cement plants, power stations, iron/steel industry installations, and oil refineries. However, point source capture by itself will not be able to reduce atmospheric CO₂ as ca. 50% of the anthropogenic emissions are from mobile sources.^[2] Direct air capture (DAC) may be able to aid in mitigating global CO₂ amounts originating from point source and non-point source emissions, and allow for onsite technologies for CO₂ storage or utilization (thereby eliminating the need for storage and transport infrastructure).^[2-4] DAC is also promising for capture of leaked CO₂ from carbon capture and storage point sources and/or geologic CO₂ storage sites.^[5] DAC requires capture from low concentrations of CO₂, ca. 400 ppm CO₂. In addition to DAC, efficient removal of low concentration CO₂ may be useful for other situations such as air purification in space stations and future human space environments, aircraft, submarine, and office buildings, and in medicine, e.g., anesthesia machines.^[6,7] In order to create efficient capture technologies for low concentration CO₂ environments, there is a need for new adsorbents.

Capture of CO₂ requires an effective and economic sorbent that possesses merits such as moderate CO₂-binding affinity, fast

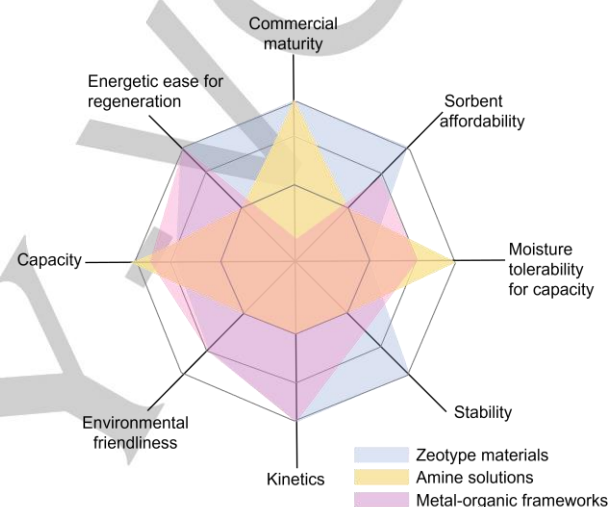


Figure 1. Radar chart illustrating some of the key features that materials need to address for use with CO₂ capture. Radar charts with other criteria are available.^[8]

sorption kinetics, high capacity, good selectivity against other components in the air, easy regeneration with minimal energy input, long-term stability, and low cost.^[8-10] In practice, all adsorbents have trade-offs, as shown in Figure 1. For instance, conventional materials like alkaline- or amine-based sorbents can effectively solve several core issues, and are currently being used by Carbon Engineering and Climeworks for DAC, respectively.^[11,12] However, they require either high temperature/energy input for regeneration or have time-dependent oxidation, and they can evaporate toxic volatiles into the atmosphere.^[2,10] Other sorbent types, such as porous materials supporting amines,^[2,13-15] moisture-swing sorbents,^[5,16] zeolites^[10,17] and metal-organic frameworks (MOFs)^[18-20] have been and are currently being investigated for CO₂ capture. Among these, zeolites and MOFs (Figure 1) are physisorbents that are showing promise for CO₂ capture because they have the potential for fast kinetics and low energy requirements for regeneration that could drastically reduce the cost of operations.^[9,10] These properties will likely be particularly significant in applications involving trace CO₂ capture, as the low concentrations of CO₂ often result in both low diffusion rates and low CO₂ capacities.^[21] Although it is challenging for these materials to maintain CO₂

RESEARCH ARTICLE

capacity under humid conditions, this can be solved by either synthesizing hydrophobic materials^[22] or engineering multi-bed systems with guard desiccant bed before the sorbents.^[23,24] Here, we focus on zeolites as they are used in many commercial applications including catalysis, adsorption and separation due to their physical and chemical stabilities.^[25–27] They can be synthesized at very large scale over a broad range of properties, e.g., very hydrophilic to very hydrophobic. Zeolites already have shown promising performance for CO₂ capture in post-combustion carbon capture processes as well as CO₂ removal in air pre-purification processes (including the international space station, where a desiccant bed is used prior to the zeolite bed for CO₂ capture).^[9,23,28,29]

Although numerous zeolites have been investigated for carbon capture,^[30–35] the research for capture of low concentrations of CO₂ (ca. 400 ppm) is scarce, and has mainly been focused on low-silica zeolites of the FAU-type (Si/Al less than 2).^[10,17,36] Low-silica zeolites have high H₂O affinity as well as low hydrothermal stability that likely will present challenges for large scale commercialization of carbon capture technologies.^[37] Here, we report a successful design of zinc exchanged CHA-type zeolites (Figure 2a) with elevated Si/Al that give higher CO₂ capacity, faster adsorption kinetics, and lower desorption energy for both CO₂ and H₂O than the standard 13X (FAU-type with Si/Al=1.1). SSZ-13 zeolites (synthetic CHA-type) were prepared, as they can be synthesized over a very broad range of Si/Al and are commercially available at several Si/Al.^[38,39] Also, SSZ-13 has demonstrated promising CO₂ adsorption performance and CO₂/N₂ selectivity for capturing high concentration CO₂.^[40–48] We demonstrate here that the choice of the zeolite as well as the state and location of zinc ions are crucial for the CO₂ adsorption performance. We denote zinc as Zn throughout, but want to make it clear that this notation does not imply zinc metal. All zinc analyzed in this study is in the form of an ion (there are several types).

Results and Discussion

CO₂ adsorption in Zn-CHA-type zeolites

CHA-type zeolites possess the CHA framework topology (Figure 2a) that consists of CHA cages connected via double six-membered rings (D6MRs), and have small pores (those that are constructed from 8 T-atoms (Si +Al) and 8 oxygen atoms – denoted an 8-membered ring, 8MRs).^[49] Here, CHA-type materials were synthesized with different Si/Al ratios (see physicochemical properties in Figures S1-S5 and Table S1). The samples were denoted as M-CHAR-NW, where M, R and N indicate the extra-framework cation type, Si/Al ratio, ion concentrations of aqueous solutions and samples washed with a copious amount of H₂O after ion exchange, respectively. If W is not included, the material was not washed with distilled H₂O after ion exchange, and if no value is listed after W, then only one exchange was performed. Column breakthrough experiments (see details in Figure S6) in a fixed-bed were used to examine the CO₂ capture performance, as this method provides breakthrough capacity, saturation capacity and diffusion kinetics, as well as desorption energy when coupled with temperature programmed desorption (TPD).

Alkali-ion containing SSZ-13 zeolites have been shown to adsorb CO₂ due to the strong electric field and acid-base

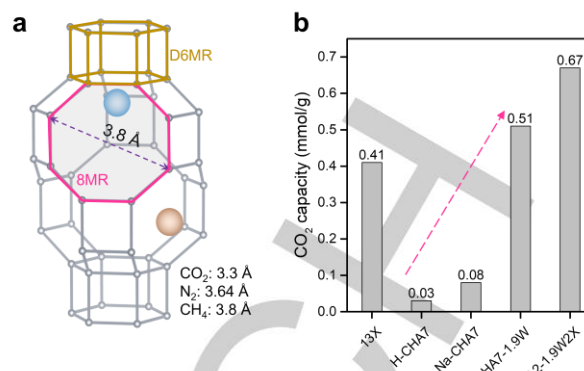


Figure 2. Performance of zinc ion exchanged CHA-type zeolites for CO₂ adsorption. a) CHA cage with 8-membered ring (8MRs) and double 6-membered ring (D6MR) highlighted in pink and gold, respectively. Extra-framework cation locations are shown by brown and blue spheres in the 8MR and below the D6MR, respectively. b) The capacities for CO₂ adsorption in ion-exchanged CHA-type (M-CHAR-NW2X) zeolites, where M, R and N indicate the extra-framework cation type, Si/Al ratio and ion concentrations of aqueous solutions, respectively. If W is not included, the material was not washed with distilled H₂O after ion exchange, and if no value is listed after W, then only one exchange was performed. Zeolite 13X is used for comparison since it is a standard and top-performing zeolite adsorbent for direct air capture (DAC).

interaction induced by the ions.^[32,44] Our results (Figure 2b) show that Na-CHA7-0.5 gives a two-fold increase of CO₂ capacity over the H-CHA7 zeolite. In order to test the effect of the varying number of ions in the solids on adsorption capacity, Na-CHA zeolites with different Si/Al ratios were investigated. The adsorption capacity (Table S2) for the zeolites with Si/Al ratios of 2, 5, 7, 9 and 20 are all substantially lower (0.16 mmol/g or less) than that of the 13X zeolite (0.40-0.41 mmol/g). Note that 13X zeolite has reported values in the literature of 0.40-0.41 mmol/g for CO₂ concentrations between 395-500 ppm, validating the reliability of our method.^[7,17,36]

As it was not possible to obtain high CO₂ capacity using Na-CHA zeolites, alternative cation types were investigated for CO₂ adsorption in CHA-type zeolites. Several ions exchanged into CHA-type zeolites exhibited increased CO₂ adsorption capacities as shown in Figure S7 and Table S2. Specifically, Zn, Nickel (Ni) and Indium (In) ions exchanged into H-CHA7 show CO₂ capacities of 0.17, 0.14 and 0.08 mmol/g, respectively. The CO₂ capacity of Zn-CHA7-0.5 (Figure S8) is increased to 0.28 mmol/g by simply washing the materials after ion-exchanged (denoted as Zn-CHA7-0.5W). An increased CO₂ capacity of 0.51 mmol/g (Figure 2b) was resulted for Zn-CHA7-1.9W, and the value is larger than that obtained from 13X zeolites. The CO₂ capacities are a function of the Si/Al ratios of the CHA-type zeolites (Figure S9), as more Zn ions can be exchanged into lower Si/Al frameworks. Successful synthesis of CHA-type zeolite with Si/Al=2 (details in Supporting Information) and then ion exchanged to give Zn-CHA2-1.9W2X shows the highest CO₂ capacity of 0.67 mmol/g (Figure 2b). This substantial increase in adsorption capacity may be useful for applications that involve multi-bed system with dried inputs to the CO₂ capture adsorbents (as described above). Zn-CHA zeolites have been reported for CO₂ adsorption at higher pressure.^[43,48] However, a lower

RESEARCH ARTICLE

adsorption capacity was observed for Zn-CHA compared to its H-form counterpart.^[43] This seemingly contrary result to the data obtained here at low concentration of CO₂ could be due to differences in the preparation of Zn containing zeolites. In order to better understand the structural features that provide the high adsorption capacity observed in this work, the active sites for CO₂ adsorption were investigated and discussed below.

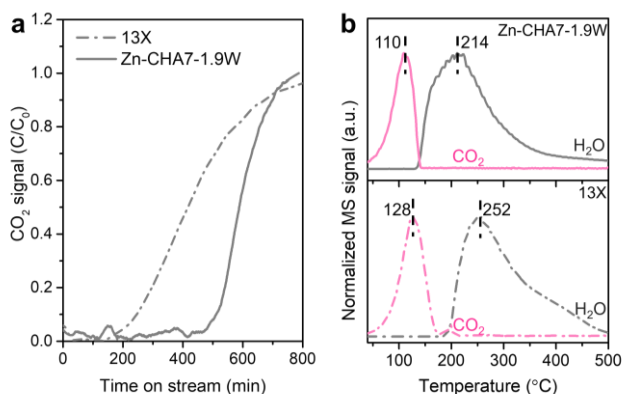


Figure 3. Comparison of gas sorption behavior of 13X and Zn-CHA zeolites. a) Column breakthrough profiles of 13X and Zn-CHA7-1.9W zeolites for the adsorption of dry CO₂. b) Temperature programmed desorption profiles of CO₂ and H₂O from Zn-CHA7-1.9W and 13X zeolites after saturation with humid CO₂ (relative humidity= 49%). The composition of the CO₂ gas for adsorption under both dry and humid conditions is ca. 400 ppm CO₂/400 ppm Ar (internal standard)/ He. Desorption experiments were performed with a ramp rate of 10 °C/min to 500 °C under 5% Ar/He gas stream.

The Zn-CHA-type materials exhibit faster adsorption kinetics than 13X, as illustrated by the sharper breakthrough profile for Zn-CHA7-1.9W compared to 13X (Figure 3a). This results in a smaller difference between breakthrough and saturation capacities. Similar results were observed for all Zn-CHA zeolites (physicochemical properties in Table S3) studied in this work (Figures S10-S11). Furthermore, a lower desorption energy of CO₂ was observed for Zn-CHA7-1.9W than 13X (Figure S12 and Table S4). Fourier-transform infrared (FTIR, Figure S13) spectra reveal that CO₂ molecules are exclusively physisorbed in Zn-CHA zeolites. However, besides physisorbed CO₂ molecules, chemisorbed, carbonate-like species are observed in 13X zeolite.^[17,50] Indeed, multicycle experiments (Figure S14) suggest that Zn-CHA zeolites show high recyclability (>80%) at temperatures as low as 60 °C under ambient pressure, while low recyclability is reported in 13X when the temperature is lower than 261 °C due to its high affinity to CO₂.^[17] Moreover, TGA results (Figure S15) show that the Zn-CHA7 zeolite adsorbs less H₂O (12.51 wt%) than 13X (19.78 wt%) after equilibrating under the same humid environments (ca. 20 % relative humidity), suggesting the former possesses higher hydrophobicity. Zn-CHA zeolite also gives promising performance for 400 ppm CO₂ adsorption under a gas stream with 49% relative humidity. Specifically, Zn-CHA7-1.9W exhibits 1.5 times breakthrough CO₂ capacity (0.22 mmol/g) of that for 13X (0.15 mmol/g), while their saturation capacities are comparable (0.22 mmol/g). Due to the weaker affinity to CO₂ (Figures S12-S13) and H₂O (Figure S15), Zn-CHA7-1.9W shows lower desorption temperature maxima

(Figure 3b) for both CO₂ and H₂O than 13X, indicating the potential of utilizing the former in a single bed adsorption system for certain circumstances. We are currently exploring further the competitive behavior of CO₂ and H₂O with the Zn-CHA materials as there are many different adsorption and desorption situations that may be applicable to commercial application.

Adsorption sites in Zn-CHA-type zeolites

Table 1. Chemical compositions and CO₂ capacities of the H-form CHA zeolites as well as the representative Zn-CHA7 and Zn-CHA(K)7 samples.

Samples	Zn/Al ^b	Si/AlOH (mmol/g) ^c	Zn ²⁺ /U.C. ^d	Zn(OH) ⁺ /U.C. ^d	CO ₂ /U.C.
H-CHA7	0.00	1.26	0.00	0	0.06
Zn-CHA7-0.002W ^a	0.08	1.10	0.21	0.12	0.27
Zn-CHA7-0.015W ^a	0.23	0.82	0.54	0.44	0.55
Zn-CHA7-0.02W ^a	0.29	0.73	0.54	0.67	0.60
Zn-CHA7-1.9W	0.54	0.33	0.96	1.64	1.21
Zn-CHA7-0.5W	0.87	0.11	0.36	3.56	0.69
H-CHA(K)7	0	1.25	0	0	-
Zn-CHA(K)7-1.9W2X	0.31	0.55	1.19	0.28	0.64

[a] Ion exchange experiments were performed in Zn²⁺ aqueous solution with pH adjusted to 4.92 by adding 0.1 M HCl aqueous solution. If not labeled, pH was uncontrolled for those materials during ion exchanges. [b] Elemental analysis was performed using EDS. [c] Concentration of Brønsted acidic protons (SiOHAl) calculated from the ¹H MAS NMR spectra. [d] Zn²⁺ or Zn(OH)⁺ ions per unit cell SSZ-13 calculated from the EDS results and SiOHAl density. More information can be found in Tables S6 and S8 in Supporting Information.

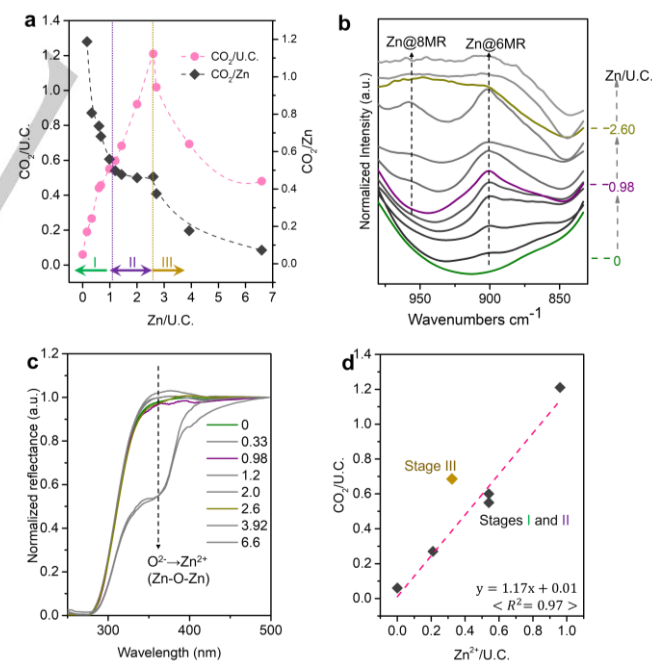


Figure 4. Speciation of Zn ions in the CHA-type zeolites and the impact on CO₂ adsorption. a) CO₂ capacity per unit cell (CO₂/U.C.) of Zn-CHA7 samples with increasing Zn ion density (Zn/U.C.). Adsorption was performed at 30 °C with a gas mixture of 400 ppm CO₂/400 ppm Ar (internal standard)/He. b) The FT-IR spectra for the framework T-O-T vibration of Zn-CHA7 materials with various Zn ion loading. c) UV-Vis diffuse reflectance spectra of Zn-CHA7 zeolites with

RESEARCH ARTICLE

various Zn ion loading. d) Correlation of the number of Zn²⁺ and CO₂ per unit cell. Dashed lines are interpolations to guide the eye.

A series of Zn-CHA7 samples were prepared with fixed Al composition (Si/Al=7) and Zn/U.C. ranging from 0 to 6.60 (Table 1 and S5), where Zn/U.C. denotes the number of Zn ions per CHA unit cell, *i.e.*, Zn ion density. As shown by the data in Figure 4a, a volcano shape profile with three distinct stages was observed. CO₂ capacity increases at two different rates (stage I and stage II) before declining when the Zn ion loading is higher than *ca.* 2.60 Zn/U.C. Simultaneously, the adsorption efficiency, *i.e.*, CO₂ per Zn ion, gradually decreases with the increase of Zn ion loading. Nitrogen physisorption results show that the micropore volume of parent CHA7 is 0.24 cm³/g, being consistent with previously reported values of SSZ-13.^[35] The micropore volumes declines upon loading of Zn ions, and comparable micropore volumes (0.18-0.21 cm³/g, Table S3) are obtained for Zn-CHA7 with Zn ion density lower than 6.60/U.C. Thus, the distinct behaviors at the three stages, as well as the variations of CO₂ capacities, are due to the speciation of Zn ions. The environments and states of Zn ions were examined to understand the CO₂ adsorption behavior. As shown in Figure 4b, two new FTIR features are seen at *ca.* 902 and 950 cm⁻¹ for the Zn-CHA7 samples in comparison to H-CHA7 (Zn/U.C.=0). These vibrations are assigned to perturbed T-O-T structural vibrations in the vicinity of extra-framework cations occupying sites in the 6MRs and 8MRs in the CHA cage, respectively.^[51-53] The observed locations of Zn ions are consistent with the results from the recent single crystal X-ray structural analysis of Zn ion exchanged large natural CHA, which demonstrates Zn ions sit in the 6MRs (outside of the D6MRs) and the CHA cage (near the 8MRs).^[54] Notably, only one band at 902 cm⁻¹ appears for Zn-CHA samples at stage I followed by the evolution of an extra band at 950 cm⁻¹ at stage II (Zn/U.C. >1.21). These results suggest that the Zn ions are exclusively located in the 6MRs at stage I, and that further increase of the Zn ion loading results in the addition of Zn ions to the 8MRs. The UV-Vis diffuse reflectance (Figure 4c) results show the formation of Zn-O-Zn species solely at stage III with high Zn ion loadings,^[55,56] as suggested by the appearance of the O²⁻→Zn²⁺ ligand-to-metal charge transfer transition band at *ca.* 360 nm.^[57] Thus, Zn ions are incorporated as Zn²⁺ and/or Zn(OH)⁺ ions (Figures S16-21, with detailed discussion in Supporting Information) at stages I and II, consistent with previous research on copper ion exchange into CHA-type zeolites.^[58]

Quantitative analysis of the state of Zn ions (Tables 1 and S6) suggests that Zn²⁺ ions are the predominant species at stage I (Zn/Al ≤ 0.23) that shows high adsorption efficiency, *i.e.*, CO₂/Zn. Correlation of the numbers of Zn²⁺ and CO₂/U.C. gives a linear relation (Figure 4d) at stages I and II. These results are consistent with Zn²⁺ being the primary adsorption site. Divalent ions (M²⁺) are known to balance the paired anionic sites introduced by the paired aluminum (2Al) sites in zeolites. Previous studies show that the 2Al sites are preferentially located in the 6MRs in the CHA cages, for SSZ-13 zeolites that are synthesized using methods similar to this work with Na⁺ as the inorganic mineralizer.^[59,60] Co²⁺ titration of the density of the 2Al sites in 6MR (Table S7) shows a Co²⁺/Al of 0.20±0.02 for the CHA7 zeolites, fitting the predicted value from the literature.^[59] Importantly, the highest value of Zn²⁺/Al obtained in the CHA7 is *ca.* 0.20, which is in good agreement with the Co²⁺/Al. Therefore, we put forth the model where (see detailed

discussion in Supporting Information) the Zn²⁺ ions responsible for the adsorption of CO₂ are located in the 6MRs in the CHA cage (as observed from the single crystal X-ray structural solution^[54]). Additionally, Zn-O-Zn is likely an extra site for CO₂ adsorption, as it is the only new species appearing at stage III with CO₂/U.C. vs. Zn²⁺/U.C. sitting above (Figure 4d) the linear correlation.

To assess if Zn²⁺ ions in the 6MRs are significant for CO₂ adsorption, further study was performed using K⁺ directed SSZ-13 zeolites (Si/Al= *ca.* 7, denoted as CHA(K)7) with 2Al dominated in the 8MRs (Figures S22-S28 and Table S8, with detailed discussion in Supporting Information).^[60] ¹H NMR results (Table 1) show comparable proton densities for the proton form of CHA(K)7 (1.25 mmol/g) and CHA7 (1.26 mmol/g). Analysis of the residual H⁺ density (Figure S24) of the Zn-CHA(K)7 zeolites indicates that each Zn ion consumes two H⁺ in the 8MRs. In contrast, close to one H⁺ is replaced by each Zn ion in the 8MRs of the Zn-CHA7 counterpart (Figure S19), and the value is two for Zn ion loaded to the 6MRs. These results suggest that Zn-CHA(K)7 zeolites contain Zn²⁺ primarily in the 8MRs, which allows a side-by-side comparison with the Zn-CHA7 materials with Zn²⁺ ions in the 6MRs to examine the significance of the location of Zn²⁺ for CO₂ adsorption. Surprisingly, the adsorption results show that CO₂ capacity remained almost constant when loading Zn²⁺ ions in the 8MRs (Figures S26). Quantification analysis (Table 1 and S27) shows that locating Zn²⁺ ions in the 8MRs with 1.19 Zn²⁺/U.C. only adsorbs 0.64 CO₂/U.C. This is markedly lower than the 1.21 CO₂/U.C. obtained for Zn-CHA zeolites with 0.96 Zn²⁺/U.C. in the 6MRs (Table 1). An adsorption efficiency of 0.65 CO₂/Zn (Table S8) was observed for Zn-CHA(K)7 with Zn(OH)⁺ dominated in the 6MRs, suggesting that a limited fraction of Zn(OH)⁺ species located in the 6MRs are able to adsorb CO₂. This could be attributed to the heterogeneous nature of the Al sites in CHA cages, leading to different environments/energies for the same extra-framework species.^[27] However, all of the Zn²⁺ in the 6MRs could adsorb CO₂ with an efficiency of 1.17 CO₂/Zn²⁺ (Figure 4d). This result would lead to the conclusion that the Zn²⁺ ions in the 8MRs are likely inactive or less effective than those located at the 6MRs, and thus highlighting the significance of locating Zn²⁺ species in the 6MRs for high CO₂ adsorption capacity. Collectively, these results show that Zn²⁺ ions in the 6MRs are the primary sites for CO₂ adsorption. This explains the observed positive correlation (Figure 2b) between CO₂ capacity and Al content in the Zn-CHA7 and Zn-CHA2 zeolites, as the latter have more 2Al (Table S1 and Figure S5) in the 6MRs that can accommodate more Zn²⁺.^[59] In contrast, Zn-CHA5 (Table S2) adsorbs less CO₂ than Zn-CHA7 due to the lower number of 2Al in CHA5 (Table S1 and Figure S5). Therefore, the Al distribution in the framework with maximizing Al located in 6MRs as 2Al sites has a critical effect on the enhanced CO₂ adsorption performance.

In order to assist in verifying the significance of 2Al sites as well as their locations in zeolites for accommodating Zn²⁺ ions for CO₂ adsorption, two groups of zeolites were selected (Figure 5). Group I (Figure S29) is small-pore zeolites with framework topologies more like the CHA-type. Group II (Figure S30) includes the standard low-silica zeolite adsorbents, namely FAU-type (13X) and LTA-type (zeolite A). As shown in Figure 5, Zn ion exchange in zeolites from group I (AEI, AFX) shows increased capacities for CO₂ adsorption. This is attributed to the presence of abundant 6MRs in these frameworks that can preferentially accommodate the divalent ions (Zn²⁺), as shown in previous studies of copper ion exchanged AEI^[61] and AFX^[62]. For group II,

RESEARCH ARTICLE

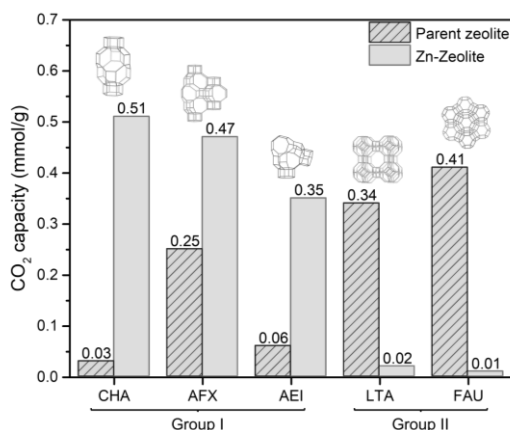


Figure 5. Zeolite topology-dependent CO₂ adsorption. Groups I is small-pore zeolites with framework topologies more like the CHA-type. Group II includes the standard low-silica zeolite adsorbents. Adsorption experiments were performed at 30 °C with a gas mixture of 400 ppm CO₂/400 ppm Ar (internal standard)/He.

the addition of Zn ions surprisingly prohibits the adsorption of CO₂ in these zeolites. These results are consistent with those from higher pressure (>0.66 mbar) adsorption where CO₂ capacity decreased with the addition of Zn ions into 13X.^[30] The significant decline in CO₂ adsorption is corroborated by the negligible absorption in the CO₂ vibration region as shown in the FTIR spectra (Figures S31 and S32). This observation could be attributed to the preferential location of divalent ions inside sodalite (SOD) cages or in the center of the hexagonal prism D6MRs in these materials (Figure S30 with detailed discussion) that are inaccessible to CO₂ molecules.^[30,63] These results altogether indicate that the framework topology and thus the positioning of extra-framework cations dictate their CO₂ adsorption properties. Specifically, the lack of SOD cages and the abundance of accessible 6MRs are two crucial factors for CO₂ adsorption in the Zn ion exchanged zeolites.

Conclusion

The addition of Zn cations into CHA-type zeolites, e.g., SSZ-13, produced greatly enhanced performance for adsorbing low concentrations of CO₂. The Zn ion containing zeolites exhibited higher CO₂ capacity, faster kinetics, lower desorption energy than the standard low-silica 13X zeolites. Control of the state and location of Zn ions in the CHA cages was crucial to the high CO₂ adsorption capacity. Zn²⁺ ions located at the 6MRs of SSZ-13 with Si/Al = ca. 7 gave an adsorption capacity of 0.51 mmol CO₂/g-zeolite, a 17-fold increase compared to the parent H-form. Lowering the Si/Al to ca. 2 resulted in an increase of capacity to 0.67 mmol CO₂/g-zeolite. Investigating zeolites with different topologies further highlights that the position of divalent ions plays a significant role in the enhancement of the capacity for CO₂ adsorption. The results presented here suggest that Zn ions exchanged CHA and several other small-pore zeolites are interesting physisorbents that merit further investigation for the capture of CO₂ from low concentration environments that may include DAC.

Acknowledgements

This work was financially supported by Carbon Capture, Inc. Y.P. would like to thank Kwanjeong Eduional Foundation for the financial support. The authors acknowledge Dr. Stacey I. Zones (Chevron) for providing chemicals for the synthesis of the AFX-type zeolite. Faisal Alshafei (California Institute of Technology) is thanked for synthesizing the OSDA for the synthesis of the AEI-type zeolite.

Conflicts of Interest

A US patent (application No. 63154334) related to this work has been applied by D. Fu and M. E. Davis as co-inventors. M. E. Davis is a consultant for Carbon Capture, Inc.

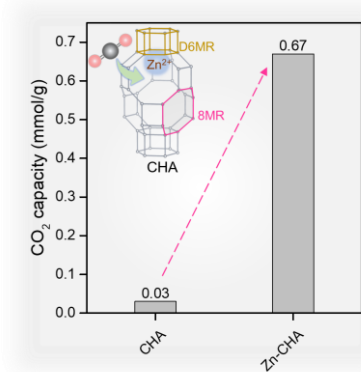
Keywords: adsorption • carbon capture • physisorbents • small-pore zeolites • zinc

- [1] K. S. Lackner, S. Brennan, J. M. Matter, A.-H. A. Park, A. Wright, B. van der Zwaan, *Proc. Natl. Acad. Sci.* **2012**, *109*, 13156–13162.
- [2] E. S. Sanz-Pérez, C. R. Murdock, S. A. Didas, C. W. Jones, *Chem. Rev.* **2016**, *116*, 11840–11876.
- [3] C. Brady, M. E. Davis, B. Xu, *Proc. Natl. Acad. Sci.* **2019**, *116*, 25001–25007.
- [4] C. Breyer, M. Fashihi, C. Bajamundi, F. Creutzig, *Joule* **2019**, *3*, 2053–2057.
- [5] X. Shi, H. Xiao, H. Azarabadi, J. Song, X. Wu, X. Chen, K. S. Lackner, *Angew. Chem. Int. Ed.* **2019**, *59*, 6984–7006. *Angew. Chem.* **2019**, *132*, 7048–7072.
- [6] O. Shekhah, Y. Belmabkhout, Z. Chen, V. Guillermin, A. Cairns, K. Adil, M. Eddaoudi, *Nat. Commun.* **2014**, *5*, 4228.
- [7] S. Mukherjee, N. Sikdar, D. O’Nolan, D. M. Franz, V. Gascón, A. Kumar, N. Kumar, H. S. Scott, D. G. Madden, P. E. Kruger, B. Space, M. J. Zaworotko, *Sci. Adv.* **2019**, *5*, eaax9171.
- [8] R. L. Siegelman, E. J. Kim, J. R. Long, *Nat. Mater.* **2021**, *20*, 1060–1072.
- [9] S. Choi, J. H. Drese, C. W. Jones, *ChemSusChem* **2009**, *2*, 796–854.
- [10] A. Kumar, D. G. Madden, M. Lusi, K.-J. Chen, E. A. Daniels, T. Curtin, J. J. Perry, M. J. Zaworotko, *Angew. Chem. Int. Ed.* **2015**, *54*, 14372–14377. *Angew. Chem.* **2015**, *127*, 14580–14585.
- [11] H. Azarabadi, K. S. Lackner, *Appl. Energy* **2019**, *250*, 959–975.
- [12] M. Fashihi, O. Efimova, C. Breyer, *J. Clean. Prod.* **2019**, *224*, 957–980.
- [13] S. A. Didas, S. Choi, W. Chaikittisilp, C. W. Jones, *Acc. Chem. Res.* **2015**, *48*, 2680–2687.
- [14] J. J. Lee, C.-J. Yoo, C.-H. Chen, S. E. Hayes, C. Sievers, C. W. Jones, *Langmuir* **2018**, *34*, 12279–12292.
- [15] A. R. Sujan, S. H. Pang, G. Zhu, C. W. Jones, R. P. Lively, *ACS Sustain. Chem. Eng.* **2019**, *7*, 5264–5273.
- [16] M. Oschatz, M. Antonietti, *Energy Environ. Sci.* **2018**, *11*, 57–70.
- [17] S. M. W. Wilson, F. H. Tezel, *Ind. Eng. Chem. Res.* **2020**, *59*, 8783–8794.
- [18] P. M. Bhatt, Y. Belmabkhout, A. Cadiau, K. Adil, O. Shekhah, A. Shkurenko, L. J. Barbour, M. Eddaoudi, *J. Am. Chem. Soc.* **2016**, *138*, 9301–9307.
- [19] K. Sumida, D. L. Rogow, J. A. Mason, T. M. McDonald, E. D. Bloch, Z. R. Herm, T.-H. Bae, J. R. Long, *Chem. Rev.* **2012**, *112*, 724–781.
- [20] D. M. D’Alessandro, B. Smit, J. R. Long, *Angew. Chem. Int. Ed.* **2010**, *49*, 6058–6082. *Angew. Chem.* **2010**, *122*, 6194–6219.
- [21] J. Liu, Y. Wei, Y. Zhao, *ACS Sustain. Chem. Eng.* **2019**, *7*, 82–93.
- [22] M. Ding, R. W. Flaig, H.-L. Jiang, O. M. Yaghi, *Chem. Soc. Rev.* **2019**, *48*, 2783–2828.
- [23] R. Kay, *SAE Trans.* **1998**, *107*, 514–522.
- [24] G. E. Cmarik, J. C. Knox, *CO₂ Removal for the International Space Station – 4-Bed Molecular Sieve Material Selection and System Design*, 49th International Conference on Environmental Systems, Massachusetts, Boston, **2019**.
- [25] E. M. Flanigen, R. W. Broach, S. T. Wilson, in *Zeolites in Industrial Separation and Catalysis* (Ed.: S. Kulprathipanja), Wiley-VCH, Weinheim, **2010**, pp. 1–26.
- [26] Y. Li, L. Li, J. Yu, *Chem* **2017**, *3*, 928–949.
- [27] M. E. Davis, *Nature* **2002**, *417*, 813–821.
- [28] K. T. Chue, J. N. Kim, Y. J. Yoo, S. H. Cho, R. T. Yang, *Ind. Eng. Chem. Res.* **1995**, *34*, 591–598.

RESEARCH ARTICLE

- [29] S. Sircar, W. C. Kratz, *Removal of Water and Carbon Dioxide from Air*, **1981**, US4249915A.
- [30] A. Khelifa, Z. Derriche, A. Bengueddach, *Microporous Mesoporous Mater.* **1999**, *32*, 199–209.
- [31] V. P. Shiralkar, S. B. Kulkarni, *Zeolites* **1985**, *5*, 37–41.
- [32] K. S. Walton, M. B. Abney, M. Douglas LeVan, *Microporous Mesoporous Mater.* **2006**, *91*, 78–84.
- [33] T.-H. Bae, M. R. Hudson, J. A. Mason, W. L. Queen, J. J. Dutton, K. Sumida, K. J. Micklash, S. S. Kaye, C. M. Brown, J. R. Long, *Energy Environ. Sci.* **2012**, *6*, 128–138.
- [34] Y. Zhou, J. Zhang, L. Wang, X. Cui, X. Liu, S. S. Wong, H. An, N. Yan, J. Xie, C. Yu, P. Zhang, Y. Du, S. Xi, L. Zheng, X. Cao, Y. Wu, Y. Wang, C. Wang, H. Wen, L. Chen, H. Xing, J. Wang, *Science* **2021**, *373*, 315–320.
- [35] J. A. Thompson, S. I. Zones, *Ind. Eng. Chem. Res.* **2020**, *59*, 18151–18159.
- [36] N. R. Stuckert, R. T. Yang, *Environ. Sci. Technol.* **2011**, *45*, 10257–10264.
- [37] N. S. Wilkins, J. A. Sawada, A. Rajendran, *Adsorption* **2020**, *26*, 765–779.
- [38] J. H. Kwak, R. G. Tonkyn, D. H. Kim, J. Szanyi, C. H. F. Peden, *J. Catal.* **2010**, *275*, 187–190.
- [39] I. Bull, W.-M. Xue, P. Burk, R. S. Boorse, W. M. Jaglowski, G. S. Koerner, A. Moini, J. A. Patchett, J. C. Dettling, M. T. Caudle, *Copper CHA Zeolite Catalysts*, **2009**, US7601662B2.
- [40] T. D. Pham, Q. Liu, R. F. Lobo, *Langmuir* **2013**, *29*, 832–839.
- [41] M. R. Hudson, W. L. Queen, J. A. Mason, D. W. Fickel, R. F. Lobo, C. M. Brown, *J. Am. Chem. Soc.* **2012**, *134*, 1970–1973.
- [42] J. Shang, G. Li, R. Singh, Q. Gu, K. M. Nairn, T. J. Bastow, N. Medhekar, C. M. Doherty, A. J. Hill, J. Z. Liu, P. A. Webley, *J. Am. Chem. Soc.* **2012**, *134*, 19246–19253.
- [43] M. Sun, Q. Gu, A. Hanif, T. Wang, J. Shang, *Chem. Eng. J.* **2019**, *370*, 1450–1458.
- [44] J. Zhang, R. Singh, P. A. Webley, *Microporous Mesoporous Mater.* **2008**, *111*, 478–487.
- [45] M. Debost, P. B. Klar, N. Barrier, E. B. Clatworthy, J. Grand, F. Lainé, P. Brazda, L. Palatinus, N. Nesterenko, P. Boullay, S. Mintova, *Angew. Chem. Int. Ed.* **2020**, *59*, 23491–23495. *Angew. Chem.* **2020**, *132*, 23697–23701.
- [46] J. K. Bower, D. Barpaga, S. Prodingler, R. Krishna, H. T. Schaeff, B. P. McGrail, M. A. Derewinski, R. K. Motkuri, *ACS Appl. Mater. Interfaces* **2018**, *10*, 14287–14291.
- [47] H. J. Kwon, S. C. Kwon, H. C. Lee, W. S. Ahn, S. H. Hong, *Carbon Dioxide Adsorbent Including Zeolite and Methods for Preparing the Same*, **2016**, US9358530B2.
- [48] T. Du, *Res. Chem. Intermed.* **2017**, 1783–1792.
- [49] M. Dusselier, M. E. Davis, *Chem. Rev.* **2018**, *118*, 5265–5329.
- [50] T. Montanari, G. Busca, *Vib. Spectrosc.* **2008**, *46*, 45–51.
- [51] J. H. Kwak, H. Zhu, J. H. Lee, C. H. F. Peden, J. Szanyi, *Chem. Commun.* **2012**, *48*, 4758–4760.
- [52] K. Mlekodaj, J. Dedecek, V. Pashkova, E. Tabor, P. Klein, M. Urbanova, R. Karcz, P. Sazama, S. R. Whittleton, H. M. Thomas, A. V. Fishchuk, S. Sklenak, *J. Phys. Chem. C* **2019**, *123*, 7968–7987.
- [53] Y. Shan, W. Shan, X. Shi, J. Du, Y. Yu, H. He, *Appl. Catal. B Environ.* **2020**, *264*, 118511–118520.
- [54] L. T. Dimowa, I. Piroeva, S. Atanasova-Vladimirova, R. Rusew, B. L. Shivachev, *Bulg. Chem. Commun.* **2018**, *50*, 114–122.
- [55] J. A. Biscardi, G. D. Meitzner, E. Iglesia, *J. Catal.* **1998**, *179*, 192–202.
- [56] A. Mehdad, R. F. Lobo, *Catal. Sci. Technol.* **2017**, *7*, 3562–3572.
- [57] N. Koike, K. Iyoki, S. H. Keoh, W. Chaikittisilp, T. Okubo, *Chem. Eur. J.* **2018**, *24*, 808–812.
- [58] E. Borfecchia, K. A. Lomachenko, F. Giordano, H. Falsig, P. Beato, A. V. Soldatov, S. Bordiga, C. Lamberti, *Chem. Sci.* **2014**, *6*, 548–563.
- [59] C. Paolucci, A. A. Parekh, I. Khurana, J. R. Di Iorio, H. Li, J. D. Albarracin Caballero, A. J. Shih, T. Anggara, W. N. Delgass, J. T. Miller, F. H. Ribeiro, R. Gounder, W. F. Schneider, *J. Am. Chem. Soc.* **2016**, *138*, 6028–6048.
- [60] J. R. Di Iorio, S. Li, C. B. Jones, C. T. Nimlos, Y. Wang, E. Kunkes, V. Vattipalli, S. Prasad, A. Moini, W. F. Schneider, R. Gounder, *J. Am. Chem. Soc.* **2020**, *142*, 4807–4819.
- [61] G. Fu, R. Yang, Y. Liang, X. Yi, R. Li, N. Yan, A. Zheng, L. Yu, X. Yang, J. Jiang, *Microporous Mesoporous Mater.* **2021**, *320*, 111060–111072.
- [62] D. W. Fickel, R. F. Lobo, *J. Phys. Chem. C* **2010**, *114*, 1633–1640.
- [63] W. P. J. H. Jacobs, J. H. M. C. van Wolput, R. A. van Santen, *Zeolites* **1993**, *13*, 170–182.

RESEARCH ARTICLE



Low concentration CO₂ is adsorbed in zinc containing CHA-type zeolites with a high capacity of 0.67 mmol CO₂/g-zeolite. The materials exhibit higher CO₂ capacity, faster kinetics, lower desorption energy than low-silica 13X zeolites. Zeolite framework and the states and locations of zinc ions play crucial roles in the adsorption performance.